

# Wettability of Commercial Polymers After Plasma Surface Treatment

P.L. SANT'ANA, J.R.R. BORTOLETO, N. C. DA CRUZ, R. P. RIBEIRO  
E. C. RANGEL, AND S. F. DURRANT

*State University of São Paulo – UNESP, Technological Plasmas Laboratory, Av.  
Três de Março 511, Alto da Boa Vista, Sorocaba, SP, 18087-180, Brazil*

In this work, the surface wettability of three commercial polymers - polyvinylchloride (PVC), polyethylene terephthalate (PET) and low density polyethylene (LDPE) - after surface treatment using SF<sub>6</sub> or N<sub>2</sub> plasmas were examined. Two techniques were tested, plasma immersion (PI) and plasma immersion ion implantation (PIII), in two distinct situations: with and without cooling of the sample holder. The water contact angle (WCA) measurements indicated that hydrophobic surfaces are obtained using fluorine plasmas ( $\theta \sim 140^\circ$ ) and hydrophilic surfaces using nitrogen plasmas ( $\theta \sim 0^\circ$ ). The high plasma temperature at an rf power of 100 W inhibits fluorine insertion, even in PIII. PI is more useful to obtain contact angles, which are stable for 30 days.

*Keywords: Plasma immersion, plasma immersion ion implantation, commercial polymers, wettability*

## 1 INTRODUCTION

The surface wettability of a solid by a liquid is a key aspect of surface science since it influences various everyday applications, including printability, anti-fogging, anti-bacterial, anti-reflection, field-effect transistor, self-cleaning windows, cookware coatings, waterproof textiles, corrosion resistance, oil-water separation and anti-bioadhesion [1–3]. When a liquid drop makes contact with a solid surface, it will either retain its drop-like shape or spread out on the solid surface. This property is characterized by using contact angle

---

\*Corresponding author: e-mail: drsantanapl@gmail.com

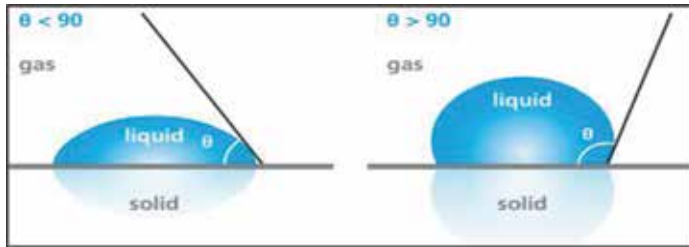


FIGURE 1

Illustration of the contact angle of a surface with: high wettability for  $\Theta < 90^\circ$  (hydrophilic surfaces); low wettability for  $\Theta > 90^\circ$  (hydrophobic surfaces).

(CA) measurements. The liquid droplet tends to form an angle with the solid surface when it is placed in contact with the solid surface. This contact angle can be measured between the horizontal line and tangential line of the liquid surface near the liquid-solid-vapor three-phase contact line. When the liquid spreads on the surface, indicating that there is affinity between the drop and the surface of the substrate, they have angles smaller than  $90^\circ$ . However, when values of contact angles are higher than  $90^\circ$ , it can be said that there was no affinity between the drop and the surface of the substrate. An intermediate situation may occur characterizing the surface as partially hydrophilic or partially hydrophobic. Figure 1 shows the drop of a liquid interacting on two different surfaces, which imply two distinct degrees of wettability, depending on  $\theta$ .

Accurate measurement of contact angles is important to characterize the surface properties of materials. Analysis of the drop shape aids the accurate measurement of the contact angle and surface tension of a liquid drop resting on a solid surface. The method involves capturing a reflected image of the drop profile, measuring coordinate points along the contour and finding the optimal mathematical fit. This represents an improvement over conventional methods, which require considerable time and can often be inaccurate. Automated equipment, however, can be very costly [4]. In the literature, it is possible to observe interesting contact angle measurements for diverse materials, including polymers [5].

The static contact angle is an indication of the balance of surface tensions between the liquid and solid ( $\gamma_{SL}$ ), liquid and gas ( $\gamma_{LV}$ ), and solid and gas ( $\gamma_{SV}$ ), as described by Equation 1, known as Young's equation [6]:

$$\gamma_{LV} \cos \theta + \gamma_{SL} = \gamma_{sv} \quad (1)$$

where  $\gamma$  represents the surface energy between the solid-vapor (SV), solid-liquid (SL) and liquid-vapor (LV) interfaces. The  $\theta$  in Young's equation is the droplet contact angle with the surface. The large contact angle implies a high

energy ( $\gamma_{SL}$ ) interface (not favorable for the liquid-solid interface), whereas a smaller contact angle implies a low energy interface (convenient liquid-solid interface). Equation (1) is only applicable to physically smooth and chemically homogeneous surfaces according to Wenzel state [7].

Moreover, among the technological methods used nowadays in commercial polymers, plasma surface treatment or deposition features some major advantages; they are fast and economical processes performed at room temperature, capable of treating complex shapes while they modify only the surface of the polymer leaving the bulk properties largely unaffected [8, 9]

Radiofrequency plasma technologies using fluorinated gases are currently employed in materials science, presenting advantages such as low-temperature reactions (in many cases the treatment can be achieved at room temperature, which avoids the thermal degradation of the material). Direct fluorination is an effective method for improving the surface properties of pristine polymer materials, including barrier properties, adhesion, printability, gas separation properties, chemical resistance, antibacterial properties (biocompatibility), etc. [10]. One of the purposes of fluorinating polymers is to increase surface hydrophobicity in polymer packaging for the food industry, leading to improvements such as greater anti-sticking, reduced friction, and flammability, reduced refractive index, low dielectric constant, and water/oil repellence properties. Improved hydrophilization is also useful since it improves adhesion in such processes as painting, coating or gluing [11].

To create hydrophobicity or hydrophilicity on polymers surfaces, Plasma Immersion or Plasma Immersion Ion Implantation [12] has emerged as a powerful tool in virtue of its simplicity and effectiveness, and can be applied for a wide number of materials [13, 14]. During the implantation, the polymer undergoes gradual compositional and structural changes and the resulting depth profile is in fact a sum of the depth distributions accumulated during various stages of the implantation process [15].

Recent literature reports the results of the modification of the hydrophobic/hydrophilic characteristics of PET [16] and PVC [17]. In those treatments, plasma immersion techniques (PI) and Plasma Immersion Ion Implantation (PIII) were employed, to modify surface wetting, roughness and optical transmission. Higher contact angles were observed after plasma fluorination and lower ones after plasma nitrogenation, while maintaining low surface roughness and high transparency in the visible, because the sample holder was at room temperature during the plasma treatment [18, 19], once high temperature effect can reduce optical transmittance in the visible range. In the present study, plasma immersion techniques were used to modify the surface properties of PVC, to increase its surface hydrophobicity or hydrophilicity using fluorine or nitrogen plasmas, respectively. Recent literature [20, 21] also reported hydrophilization on the surface of LDPE after oxygen surface plasma treatment.

Packaging has a fundamental role in ensuring safe delivery of goods throughout supply chains to the end consumer in good condition. It also has great potential to contribute to sustainable development. The increasing environmental concern among consumers in their selection of food products also seems to include the packaging as reported by Rokka and Uusitalo [22]. Packaging plays an important role in preserving, protecting and marketing products during their storage, transport and use [23]. In this sense, the introduction of new technologies could lead to a reduction of the processing time or an improvement in operating conditions, thereby decreasing both environmental and financial costs [24].

The paper introduces the results of wettability with ageing of three commercial polymers treated in warm atmosphere and cold atmosphere, and following, results of infrared spectrum and XPS are presented.

## 2 EXPERIMENTAL TECHNIQUE

The experimental setup used consists of a stainless-steel vacuum chamber (30 cm in height and 25 cm in diameter) with two horizontal circular internal electrodes of stainless-steel of 11 cm diameter. Substrates were placed on the driven or biased electrode and the system was evacuated by a rotary pump (18 m<sup>3</sup>/h) down to 0.1 Pa. Needle valves were employed to control the gas feed (both with high purity: up to 99.9995 %), and a capacitive pressure sensor to monitor the chamber pressure. PVC, PET and LDPE samples were exposed directly to the plasma environment established by the application of radiofrequency power (13.56 MHz) at 25 and 100 W for both gases (N<sub>2</sub> and SF<sub>6</sub>). There was a total of twenty four substrates of blue PVC (2.5 cm × 1.5 cm × 1 cm); eight substrates were treated to differ in each of three different RF plasma immersion modes, as summarized as follows:

- i. The sample holder and the chamber walls were grounded while rf power was connected to the opposite electrode (driven electrode): PI 'anode'; (eight samples).
- ii. The rf power was connected to the sample holder (driven electrode) while the other electrode and chamber walls were grounded: PI 'cathode'; (eight samples).
- iii. The rf power was connected to the upper electrode (driven electrode) while negative pulses of high voltage were applied to the substrate holder: PIII, (eight samples).

A high voltage source (model RUP-6) and an oscilloscope (TDS from Tektronics) were employed for the PIII experiments. The high negative voltage was -2400 V, the frequency was 300 Hz and the duty cycle, calculated as  $t_{\text{on}}/(t_{\text{on}} + t_{\text{off}})$ , was ~0.33 for  $t_{\text{on}}$  fixed to 30  $\mu\text{s}$ , for all PIII experiments. PVC,

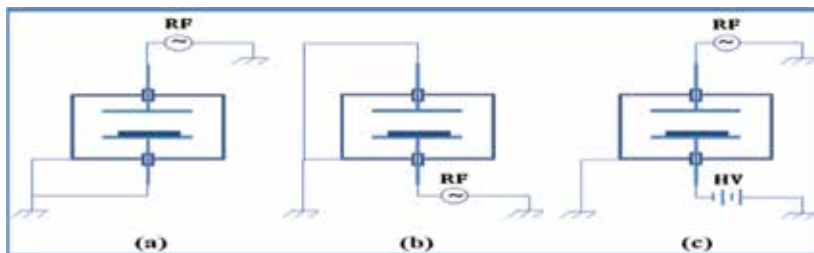


FIGURE 2  
Electrical configuration of plasma immersion techniques applied in our experiments. (a) Plasma Immersion anode; (b) Plasma Immersion cathode; (c) Plasma Immersion Ion Implantation [6-9].

PET and LDPE samples were treated with sulfur hexafluoride ( $\text{SF}_6$ ) and more twelve for nitrogen ( $\text{N}_2$ ) plasmas. Figure 2 shows the electrical configuration of the plasma immersion and plasma immersion ion implantation techniques used in our experiments.

As warming, during the process, occurred this changed the optical transmittance, immediately after the rf power was cut, the WCA was measured using a goniometer (100-00, Ramé- Hart) using three drops of deionized water, measured ten times per drop via appropriate software. The drops had a volume of  $0.6 \mu\text{l}$ , and ten measurements were made for each sample. Structural molecular groups of PVC and PET were studied by infrared spectroscopy using a Jasco 410, employing attenuated total reflectance. The effect of the plasma treatment on the chemical composition of the PVC surface was evaluated using wide energy x-ray photoelectron spectroscopy scans. Data were collected for the untreated PVC (one sample) and plasma-treated PVC (four samples). A Microtech - ESCA 3000 spectrometer was employed with a base pressure of  $2 \times 10^{-8}$  Pa, using the Mg  $K\alpha$  radiation, and achieving a resolution of about 0.8 eV. Table 1 shows the technical parameters.

### 3 RESULTS AND DISCUSSIONS

#### 3.1 PVC and PET Treatments (without Cooling System)

Water contact angles of pristine substrates are presented. Three drops were measured and the mean of 30 values is given. Table 2 shows the values with their respective standard deviations.

For the experiments (without cooling system, PVC and PET were submitted to a temperature of  $\sim 85^\circ\text{C}$ , owing to ion bombardment on the sample surfaces (neutral and ionized species) and plasma kinetics; hence Figure 3 shows values of the contact angle of PVC: 6.665 Pa of  $\text{SF}_6$  and  $\text{N}_2$  under different plasma immersion techniques for 300 s, at different rf applied power. LDPE did not resist high temperature in the plasma environment.

TABLE 1  
Plasma immersion procedure conditions for the PVC samples.

Substrates	PVC PET LDPE
PI parameters	
Gas system	SF <sub>6</sub> and N <sub>2</sub>
Base pressure (Pa)	0.1
Work pressure (Pa)	6.66
Treatment time (s)	300 to 900
rf power (W)	25 to 100
Temperature (K)	Plasma or 298
PIII parameters	
High voltage (V)	-2400
Cycle time (μs)	30
Frequency (Hz)	300

\*At 25 W, the plasma gas temperature reaches 60 °C and at 100 W the plasma temperature reaches 80 ° C. Using a sample-holder cooler system, the substrate temperature is maintained at 25 °C.

TABLE 2  
Contact angles for the pristine polymer substrates obtained by the sessile drop method at room temperature.

Pristine substrates (without treatment)	Mean values ± standard deviation (°)	
Polyvinyl chloride PVC	70 ± 4.0	[25]
Polyethylene Terephthalate PET	66 ± 5.5	[25]
Low Density Polyethylene LDPE	74 ± 1.0	[25]
Polyamide 6	62 ± 3.0	
Silicone	108 ± 10	
Natural rubber	28 ± 6.5	
Polytetrafluoroethylene (PTFE)	112 ± 5.5	[26]
Polymethylmethacrylate (PMMA)	53 ± 1.0	[27]

The results were very similar to those of PVC and PET treated under the same conditions for all rf powers and all the three plasma immersion techniques. Contact angle measurements show that the wettability depends on the plasma technique. The highest value of  $\theta \sim 130^\circ$  occurred at 100 W in fluorine plasma while the lowest  $\theta \sim 15^\circ$  in nitrogen plasma. As shown in Figure 4, the treatment by all plasma immersions changes the surface chemical structures, creating new radicals.

The PVC and PET surfaces were fluorinated, giving origin to C-F bonds. Although C-F bonds are highly polar, when these species are present on the surface of PVC and PET, they will increase its hydrophobicity. After fluorine

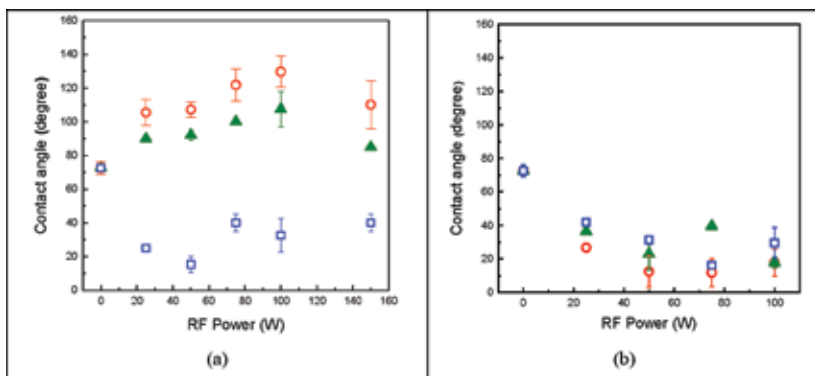


FIGURE 3

Contact angle as a function of applied rf power for PVC treated by: (a)  $\text{SF}_6$  plasma and (b)  $\text{N}_2$  plasma. The symbols on the graphs are associated with the following plasma techniques:  $\circ$  (PI cathode),  $\Delta$  (PI anode), and  $\square$  (PIII), with respective standard deviation. Temperature during the treatments was 358 K. Pressure was 6.6656 Pa of gases for 300 s at different RF Power. The parameters of PIII were -2400 V, 300 Hz and 30  $\mu\text{s}$ .

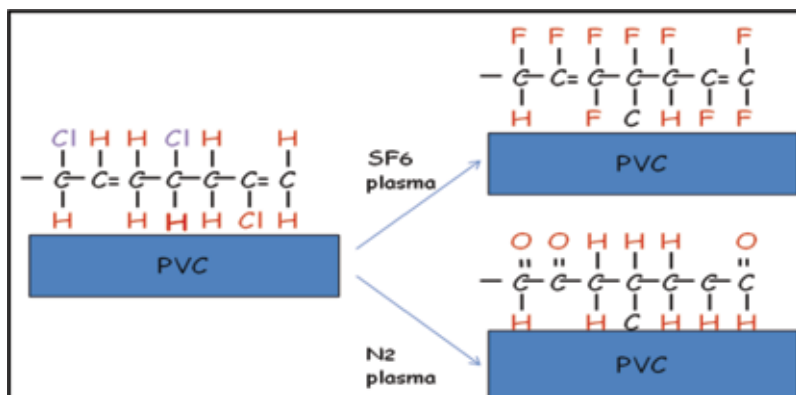


FIGURE 4

Effect of treatment on White PVC caused by plasma immersion using  $\text{SF}_6$  plasma and  $\text{N}_2$  plasma. Hydrogen atoms are displaced by fluorine or atmospheric oxygen atoms, producing CF or CO bonds.

insertion into the polymer backbone, the surface becomes hydrophobic, owing to the process of fluorination, which results in a substantial change of the chemical composition of PVC and PET. Owing to a relatively high C–F bond energy inside the fluorinated layer, most of atmospheric O, Cl or H-atoms are easily replaced by F-atoms and double bonds are saturated with fluorine to form C–F bonds on PVC.

These results decreased the surface energy, such that free radicals and dangling bonds tend to capture oxygen, especially when the sample is exposed to ambient conditions, when oxygen-containing groups and other polar radicals can recombine, and connect with the carbon backbone.

The availability of fluoride ions in plasma immersion can be a determining factor in the reorganization of molecular and free radical groups, which influences the  $\theta$  values. Owing to their high ionization energy (17.4 eV)  $F^+$  ions are hardly produced. They may be available as plasma phase clusters with charge 1, for example,  $CF_2^+$ , but not in plasmas containing pure sulfur hexafluoride.

Since the  $F^-$  ion is not attracted to the electrode with negative pulses (exclusively for the PIII treatments), this might explain the absence of a hydrophobic agent (which would be the fluoride in the implanted samples in this condition). In fact there was an increase in the hydrophilic character of the surface of the polymeric substrates after ion implantation, measured after breaking the vacuum, even in an atmosphere containing reactive fluorine. Subsequently, trapped ions diffuse to the surface [28].

The incorporation of fluorine resulted in formation of different functional groups on the surface, which can be attributed to CF, CHF,  $CF_2$ , and  $CF_3$  [25]. However, when changing the polarization of the rf power, that is, PI anode technique, there is no acceleration of ions towards samples set on the lower electrode, so this accounts for the reduction in contact angle, although samples are exposed to an  $SF_6$  plasma. It is suggested that fluorination by plasma immersion resulted in disruption of C–H bonds followed by fluorine atom addition and a tendency to saturation of double (conjugated) C=C bonds with fluorine.

In treatments using  $N_2$ , initially, 6.665 Pa of  $N_2$  was used for 300 s for rf powers from 25 W to 100 W. Parameters for PIII were –2400 V, 300 Hz and 30  $\mu$ s. For this condition, hydrophilic surfaces of PVC and PET were obtained, as summarized in previous works [28]. As already noted residual oxygen may form chemical bonds with free radicals during the plasma process. Post treatment reactions with oxygen or water vapor or both are also known to occur [25]. The concentration of CO-containing groups inside the fluorinated layer does not depend on its thickness and is increased at greater oxygen concentrations in the fluorinating mixture, even if O is provided by the ambient atmosphere after vacuum breaking. The change in the surface hydrophilicity is caused by the replacement of C–C or C–H group on the surface of PVC by C–O or C=O groups [29–33]. These radicals may take part in reactions resulting in scission of polymer chains and formation of polar groups.

It is suggested that the high energy acceleration of positive ions toward the lower electrode promotes higher rates of sputtering or etching or both. Also, the high temperature resulting from the greater bombardment can inhibit the incorporation of fluorine into the surface of polymeric substrates because it reduces the adsorption of precursor species. Thus, changes in  $\theta$  were caused



by the dynamics of adsorption and desorption on the surface, which induce compositional and structural changes. On exposure to ambient conditions, the treated surface readily incorporates oxygen or water vapor or both on active surface sites, and the high temperature acts as a catalyst for oxidation processes, which explains the reduction in  $\theta$  after PIII treatment in a heated environment.

For the  $N_2$  treatment, the combination of polar functional groups on the surface led to the hydrophilicity of the material most of the times. When polar groups such as C-OH, C-O, C=O, (C=O)-O, for example, are present on the surface and the liquid used is also polar, like deionized water, electrostatic attraction prevails. In this case, the attraction between the surface oxygen and the water hydrogen is greater than the repulsion between the oxygen atoms (surface / liquid). So the higher the proportion of oxygen on the surface, the more hydrophilic it will be. In addition, the atoms and O-groups, together, cause greater etching of polymers, mainly on the amorphous regions.

The penetration depth of such ions is only a tenth of a few nm, so they cannot cause substantial modification on the subsurface layer. Small differences in the polymer structure are reflected in different etching rates resulting in the evolution of the surface morphology for the polymeric samples. A synergic effect of ultraviolet radiation causes modification of substrate layers to a few tens of nm. The presence of O groups in the plasma phase caused etching of less resistive components of the polymer [34].

The conditions for the next series were: 6.665 Pa of  $SF_6$ , with rf power ranging from 25 to 150 W for a treatment time of 900 s on PET. Fig. 5 shows the graphs of contact angle as function of time, for measurements made immediately after removal of the samples from the reactor.

According to Figure 5(a), samples treated with  $SF_6$  become hydrophobic. The hydrophobic surface properties might be increased and stabilized owing to the replacement of C-H bonds or oxygen containing groups by C-F bonds [35] or even the incorporation of  $CF_2$  and  $CF_3$  groups onto the polymer surface after treatment [36]. It has been demonstrated that fluorination of PET surface can be achieved through fluorine radicals generated in the sulfur hexafluoride plasmas [37-38]. The mechanism of fluorination is simple, allowing appreciate the resulting hydrophobic surfaces and high values of  $\theta$ .

On the other hand Figure 5(b), shows that nitrogen plasma treatment causes oxidation of polymeric chains making the surface more hydrophilic [39]. Atmospheric oxygen is a highly reactive gas, and the plasma conditions used in the experiment completely dissociated the oxygen gas into different species inside the plasma chamber. Oxygen radicals in the plasma react with the functional groups at the surface of the PET sample causing surface etching [40], which explains the low roughness after PIII and PI treatment.

It is probable that the O incorporation immediately after treatment causes high hydrophilicity of PVC and PET, and probably of LDPE. As long as the O goes out from the polymer matrix, the tendency with aging is to become

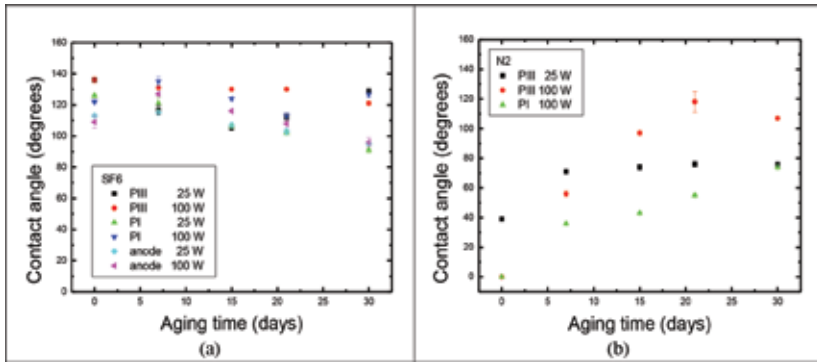


FIGURE 5

$\theta$  evolution on aging time of PET surfaces, in (a): that were exposed to 6.6656 Pa of SF<sub>6</sub>, applying rf power of 25 W and 100 W for 900 s. The parameters of PIII were: -2400 V, 30  $\mu$ s and 300 Hz. PI indicates treatments with electrode sample-holder polarized with rf, and opposite electrode grounded. In PI anode,  $\theta$  values were not as high as those of PI (cathode). And in (b), surfaces that were exposed to N<sub>2</sub> plasma for 900 s, at 25 W and 100 W of RF Power discharging PI anode experiments.

more hydrophobic. Another polymer, PVC, was also treated in the same conditions, and presented high proportions of oxygen groups as shown by FTIR and XPS analysis [25]. On the other hand, the higher fluorine contents incorporated onto the surface increases the hydrophobic character, as confirmed by the high values of  $\theta$ , which imply non-chemical attraction between the fluorinated surface and the test fluid [41].

We must remember that these results were conducted without a substrate cooling system and the temperature immediately after the treatments were averaged  $\sim$ 358 K. For instance, there is evidence of fluorination or oxidation of commercial plasmas treated at low temperature. If we treated both polymers at room temperature, would it be possible to reach higher values of  $\theta$  in fluorine plasmas, and lower values of  $\theta$  in nitrogen plasmas?

### 3.2 PET and LDPE Treatments (with Cooling System) and Infrared Analysis

Sant'Ana *et al.* [25] reported the use of continuous cooling of the sample holder at  $T \sim$ 298.2 K, as recorded using a digital thermometer. This condition, produced highly hydrophobic surfaces as confirmed by the same sessile drop method. Hence values of  $\theta$  above 150° were obtained for PVC, and above 130° for PET.

In other studies, plasma technology surface treatment of food packaging was demonstrated through surface activation, sputtering, etching, cross-linking, functionalization, film deposition or by some combination of these [42], which work in principle, allows the reuse of recycled polymeric food packaging [43].

TABLE 3

Contact angle as a function of the cycle time for PET and LDPE samples treated with (13.33 Pa) of  $N_2$  for 300 s, 25 W of RF power, 298 K for different Ion Implantation cycle times. Pulses of  $-1000$  V at 300 Hz were applied.

Cycle time ( $\mu$ s)	PET contact angle ( $^\circ$ )	LDPE contact angle ( $^\circ$ )
0 (untreated)	$70.0 \pm 15$	$76 \pm 10$
1	$51.3 \pm 10$	$30 \pm 15$
30	$46.0 \pm 15$	$24 \pm 15$
100	$31.1 \pm 20$	$17 \pm 20$
500	$19.1 \pm 10$	$9 \pm 10$

Treatments using PI and PIII at double the pressure ( $\sim 13.33$  Pa) of  $SF_6$  or  $N_2$  at rf of 25 to 100 W for 300s, at room temperature ( $\sim 298$ . K) have been made. High values of  $\theta$  were found for fluorinated surfaces and low values of  $\theta$  were found for nitrogenated surfaces. The key is: for  $SF_6$  plasma, the hydrophobic behavior of polymeric surfaces is much more stable upon ageing. Table 3 shows the results obtained in low electrode sample-holder temperature.

Recent studies associated the improvement of wettability with an increase in the concentration of oxygen groups on the PET surface after plasma treatment [44]. The changes in wettability observed after plasma treatment of polymer surfaces and after storage of the modified material are explained by mobility of the macromolecules on the top surface level [45]. Accepted models of the surface energy decrease and recovery of hydrophobicity with time in these plasma-treated polymers involve the rotation of high energy surface functional groups back into the polymer bulk. Surface energy is, thereby, reduced and hydrophobicity increased. Such rotations seem unlikely to give the highly carbonized structure associated with high fluence modification. Independently of the efficacy of the treatment, the reduction of  $\theta$ , is a transient effect, as observed in treatments of silicone surfaces [46].

In recent studies, FTIR spectral analyses indicate that the carbon content decreases and the oxygen content increases on the surface of PET and LDPE, and a large concentration of oxygenated polar functional groups is introduced into the surface by plasma treatment, which is responsible for improving its wettability [47]. Recent studies reveal the wettability issues related to PET. For example, the partial hydrophobic nature of PET results in poor uptake and adhesion of dyes, particles and microcapsules [48, 49].

Figure 6 shows infrared spectra of pristine and treated LDPE samples. The conditions stipulated for PIII were: 13.33 Pa of  $N_2$ , 25 W of RF Power for 300 s for ion implantation cycle times (in  $\mu$ s) of 1, 30, 100 and 500 at  $-2400$  V.

Although it is primarily a qualitative analytical tool, infrared spectroscopy has been used to quantitatively gauge the concentrations of functional groups

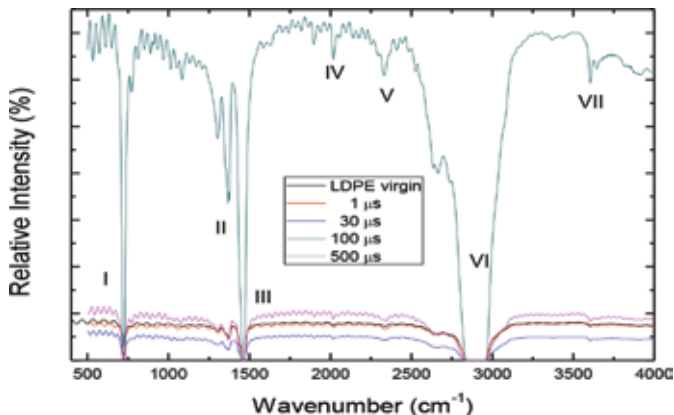


FIGURE 6

Infrared spectra of LDPE treated by PIII at 13.33 Pa of  $N_2$ , 25 W of RF Power using  $N_2$  plasmas for 300 s for ion implantation cycle times ranging from 1, 30, 100 and 500  $\mu s$  at -2400 V.

in plasma polymers and hence the crosslinking density of hydrocarbon plasma polymers [50, 51]. An absorption at  $3600\text{ cm}^{-1}$  (VII) shows the presence of  $-OH$ , on the treated surface. The residual oxygen makes chemical bonds with C or H during plasma process, and also, C and H captures oxygen from the air when the samples are exposed to the atmosphere immediately after treatment [52]. Bonds with hydrogen are weak and thus they are easily broken [53], however process at low temperature, avoids degradation of polymer substrates [54].

The position of the bands as indicated on the FTIR spectra are similar for all LDPE samples, but their intensities are slightly different, such as a strong band in  $2900\text{ cm}^{-1}$  (VI) caused by C-H stretching vibrations in  $CH_2$ . The variation is more evident at 500  $\mu s$ , in which the intensity of the peaks at  $2340\text{ cm}^{-1}$  (V)  $N-H^+$ , attributed to amine absorption and correlated compounds at  $\sim 1950\text{ cm}^{-1}$ , (IV) attributed to allenes  $-C=C=C-$  become stronger. The band at  $1490\text{ cm}^{-1}$  (III) is attributed to the C-H bending vibrations of paraffin hydrocarbon [55]. The peaks at  $1350\text{ cm}^{-1}$  (II) are attributed to an axial deformation of the C-O from carboxylic acid coupled to  $-OH$ . An absorption peaked around  $730\text{ cm}^{-1}$  (I) is attributed to angular asymmetrical in-plane deformation of  $-(CH_2)_n-$ . There are sufficient C-C, C=C, C-H, C-O and C=O bonds to explain hydrophilic surfaces.

FTIR is well-established for the elucidation of structural chemical changes [25]. Figure 7 shows an Infrared spectrum of pristine PET, in (a) for pristine PET, and in (b), for PET treated by PIII changing the high voltage.

PET exhibited fifteen molecular groups, and its structure is more complex than LDPE. In Figure 7.b a spectrum of implanted PET is showed. The  $N_2$  pressure was 13.33 Pa; the applied power 25 W, the treatment time 300s. The cycle time was 30  $\mu s$  and the applied voltage ranged from  $-500\text{ V}$  to  $-2500\text{ V}$ .

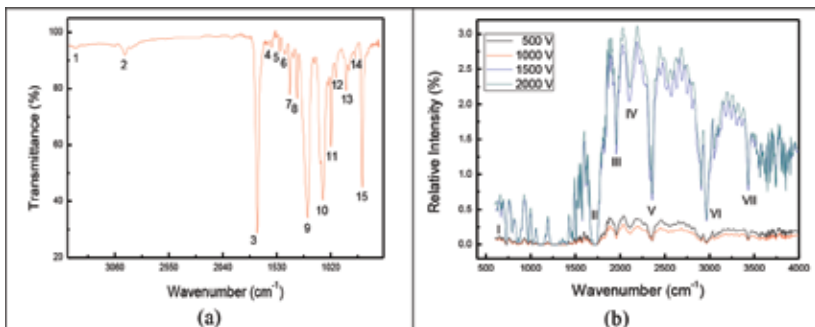


FIGURE 7

Infrared spectra of virgin PET for the identification of functional groups in (a) virgin PET (b) implanted PET. The treatment parameters were 13.33 Pa of  $N_2$  for 300 s, at 25 W for different high voltages and a cycle time of 30  $\mu$ s at 300 Hz.

The following attributions of the observed absorptions were made: Hydrogen on the aromatic ring associated with the band located in  $724\text{ cm}^{-1}$  (15), characteristic of out-of-plane vibrations; the presence of  $R_2C=CHR$  related to angular deformation of C-H out-of-plane vibration near  $792\text{ cm}^{-1}$  (14); and also at  $872\text{ cm}^{-1}$  (13) related to the angular deformation of  $R_2C=CH_2$ ; at  $970\text{ cm}^{-1}$  (12) related to the angular deformation of  $-CH=CH-$  groups; at  $1017\text{ cm}^{-1}$  (11) related to  $S=O$  (conjugated sulfoxide). An absorption caused by C-O in carboxyl ester groups is observed at  $1094\text{ cm}^{-1}$  (10), binding the O-C from the  $O-CH_2$  groups. The band located at  $1240\text{ cm}^{-1}$  (9) is caused by the stretching of C=O groups. A band located at  $1338\text{ cm}^{-1}$  (8) is associated with the asymmetric angular deformation of sulfone ( $SO_2$ ). The presence of sulfur-containing groups may indicate the presence of additives in the material or cleaning processes. In addition, more bands were detected, at  $1407\text{ cm}^{-1}$  (7), associated with the axial deformation of  $CH_2$ ; at  $1460\text{ cm}^{-1}$  (6) associated with the axial deformation of  $-(CH_2)_n$ ; at  $1504\text{ cm}^{-1}$  (5) associated with the axial deformation of N-H; at  $1580\text{ cm}^{-1}$  (4) associated with the symmetric axial in-plane deformation; at  $1715\text{ cm}^{-1}$  (3) associated with the C=O bond stretching in the carbonyl group; and also at  $2965\text{ cm}^{-1}$  (2), associated with the axial deformation of C-H (stretching), and finally, at  $3430\text{ cm}^{-1}$  (1) associated with stretching of the hydroxyl group [3, 40]. These results are reported in literature [48, 49].

After the ion implantation at low voltages ( $-500\text{ V}$  and  $-1000\text{ V}$ ), weak absorptions were generally observed, while at high voltages ( $-1500\text{ V}$  and  $-2000\text{ V}$ ), absorption increased. The band centers do not shift significantly in wavenumber. The band observed at  $740\text{ cm}^{-1}$  (I) was maintained, and is associated with the angular deformation of the chain  $-(CH_2)_n$  (for  $n>3$ ), which configures an aromatic ring. The band observed at  $1740\text{ cm}^{-1}$  (II) is associated with carbonyl groups. A new group appeared close to  $1900\text{ cm}^{-1}$

(III), associated with  $\text{-C=C-C-}$  alene. This double bond may constitute crosslinking between chains. The origin of another new band, which appears between  $2000$  and  $2200\text{ cm}^{-1}$  (IV), may be attributed to  $\text{SC}\equiv\text{N}$  (thiocyanate), to  $\text{-N=N=N}$  (azides), or to  $\text{-C=C=O-}$  (ketones). Unsaturated bonds are present in each of these possibilities. A new band at  $2340\text{ cm}^{-1}$  (V) is associated with amine groups. The band near  $2965\text{ cm}^{-1}$  (VI) is associated with  $\text{C=O}$  stretching in carbonyl groups. And finally, the band near  $3430\text{ cm}^{-1}$  (VII) is associated with stretching of the hydroxyl group. In all cases, the bands were narrow.

The presence of the new groups after ion implantation explains the hydrophilization of a shallow surface region of the material, by diffusion of water vapor and oxygen from the atmosphere. This diffusion mechanism occurs more intensely in the amorphous regions of the material, or even on the surface on which the atoms have greater mobility [25].

### 3.3 PVC Treatments (with Cooling System) and XPS Analysis

In Prestes [56] values of  $\theta$  close to  $120^\circ$  were recorded for PVC, in its best condition, at  $80\text{ W}$  for 2 minutes ( $120\text{ s}$ ), and a system pressure of ( $\sim 13.33\text{ Pa}$ ). This reveals that the high pressure combined with a moderate rf discharge power in relatively short times is capable of inducing a strong hydrophobic character on the surface of the polymers, showing that Plasma Immersion is a fast or effective technique, at a relatively low operational cost. Thus, the plasma surface treatment for the fluorination of recycled polymer surfaces should be undertaken with the sample holder at room temperature. Figure 8 shows contact angle measurements as function of the plasma immersion technique. The pressure of gases was  $66.66\text{ Pa}$ , at  $100\text{ W}$ , at room temperature ( $\sim 298\text{ K}$ ).

A high degree of fluorination was obtained, on both polymers when treated by PI or PIII with  $\text{SF}_6$  plasma; and analogously, high degree of polar groups containing O was obtained on both polymers when treated by PI and PIII with  $\text{N}_2$  plasma. A priori, the high energy of electrons and ions in the plasma can compromise the insertion of fluorine on a micro or nanometric scale. In fact, the predominance of sputtering mechanisms on the surface is compatible with the formation of sigma or double covalent bonds. It is noteworthy that the sputtering mechanism is necessary to the process, as there will only be a recombination of C with F or O, on the surface, if there are active sites (pendant C bonds on the surface). The vacuum level may not be sufficient to totally avoid the presence of contaminants, or groups containing oxygen [57].

Figure 9 shows the graph of contact angle as function of pressure of  $\text{SF}_6$  inside the reactor.

Here, it is a clear case of fluorination of polymer surfaces. For the polymers investigated in this series, the contact angle values increased with increasing pressure of  $\text{SF}_6$  in the reactor, making the surface of the substrates hydrophobic. This increase, however, was small for pressures above  $25\text{ mTorr}$  ( $\sim 3.33\text{ Pa}$ ), that is, after  $25\text{ mTorr}$  the contact angle values tend to stabilize.

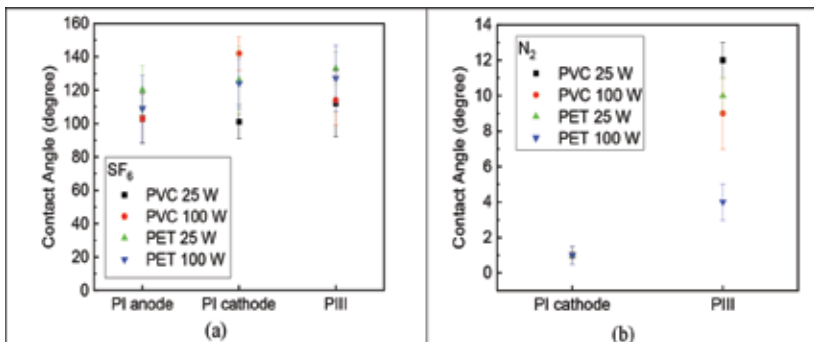


FIGURE 8

Contact angle as a function of the plasma immersion technique. The pressure of gases was 66.66 Pa, at 100 W, at room temperature ( $\sim 298$  K) in each experiment. The PIII parameters were  $-2400$  V, cycle time  $30\mu\text{s}$  at  $300$  Hz.

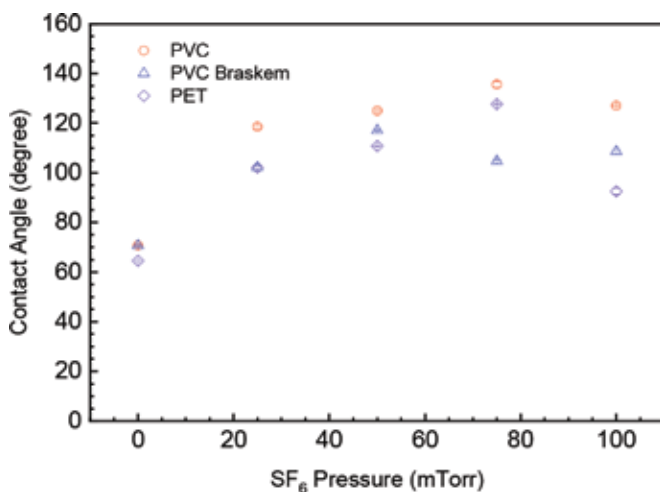


FIGURE 9

Contact angle as function of  $\text{SF}_6$  pressure: Samples of commercial white PVC, PVC from Company Braskem and PET from 2 L Coke<sup>TM</sup> bottles were treated by PI cathode at 100 W for 900 s and a temperature  $\sim 358$  K [58].

The highest value of  $\theta$  was observed for commercial PVC treated with different  $\text{SF}_6$  pressures close to  $140^\circ$ . This value is  $20^\circ$  higher than the value of  $\theta$  found in a study made under similar thermodynamic conditions [58].

In fact, even increasing the amount of gas, it is understood that, there is not enough ionized gas to chemically modify the surface, because with the increase in pressure, there is a decrease in the mean free path, thus decreasing the cross section and, consequently, the average kinetic energy of the

TABLE 4

Treatment conditions: 25 W and 100 W rf power, and 6.66 Pa of gases for 900 s. PIII parameters were -2400 V, 30  $\mu$ s and 300 Hz.

Gas	Treatment identification	Power RF (W)	Plasma configuration	Initial contact angle ( $^{\circ}$ )	Contact angle ( $^{\circ}$ ) 30 days
SF <sub>6</sub>	Pristine PVC	0	-	76 $\pm$ 10 [81, 3, 40]	76 $\pm$ 10
	Flu1	25	PIII	112 $\pm$ 10	135 $\pm$ 25
	Flu2	100	PIII	113 $\pm$ 10	131 $\pm$ 25
	Flu3	25	PI Cathode	100 $\pm$ 15	123 $\pm$ 10
	Flu4	100	PI Cathode	142 $\pm$ 20	124 $\pm$ 20
	Flu5	25	PI Anode	103 $\pm$ 10	123 $\pm$ 10
	Flu6	100	PI Anode	103 $\pm$ 10	123 $\pm$ 10
N <sub>2</sub>	Nit1	100	PIII	9 $\pm$ 20	102 $\pm$ 10
	Nit2	100	Cathode	1 $\pm$ 0.5	131 $\pm$ 20

molecules that make up the plasma [58]. Soon the availability of fluorine ions is reduced, thus decreasing the degree of fluorination of the polymers.

If until now the mechanism of changes in  $\theta$  caused by ageing is not well elucidated, here we focus on a new series of treatment of PVC at room temperature to aid our discussion of fluorination and oxygenation and their stability to 30 days. Table 4 shows the contact angle as a function of time, measured immediately after the removal of PVC samples from the reactor, and after 30 days ageing.

PVC is a slightly hydrophilic polymer with a water contact angle of around 76 $^{\circ}$   $\pm$  10 $^{\circ}$  [25, 58]. According to the data of Table 4, wettability after treatment depends on the plasma configuration. Plasma immersion using nitrogen decreases contact angles, whilst plasma immersion using fluorine increases them, independent of the plasma technique. Owing to the plasma action, the breaking of covalent chemical bonds, such as C-H or C-O and their subsequent recombination may lead to the formation of C-F bonds after the fluoride treatment by PI [25, 58] which explains the increased hydrophobic character of the polymers undergoing this treatment.

In the reactor there are also the effects of ionic bombardment for all PI configurations. In addition, as the ageing time increases,  $\theta$  gradually recovers its initial character, particularly after treatment in nitrogen plasmas. There may be a chemical evolution with time. Furthermore, we consider that the structural reorganization of the polymer chains may play an important role in hysteresis of the polymer's wettability as seen in the literature [57, 58].

XPS is more suitable for surface analysis and more quantitative than infrared spectroscopy. Under some experimental conditions, XPS detected more than 10 at. % oxygen on the treated PVC surfaces [25] but only about 2 at. % in Prestes' works [79]. It is concluded that the effect of incorporating residual



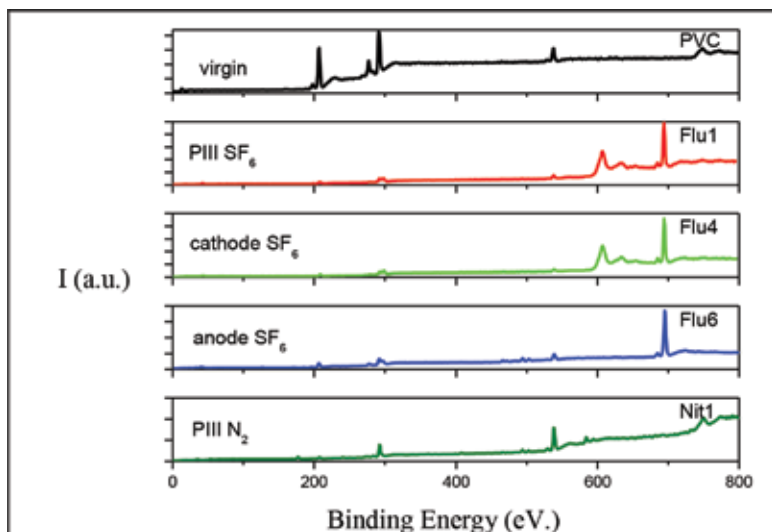


FIGURE 10

XPS spectra of untreated PVC and PVC treated under different conditions: PIII associated to fluorine or nitrogen treatment, and PI associated to fluorine treatment (cathode or anode electrical configuration), which BE ranged from 0 to 800 eV.

oxygen will always occur, in all conditions, however the fluorination mechanism is more efficient at room temperature. In addition, the process was reproducible, as in fact was confirmed, and has already been foreseen in previous works [80].

Figure 10 shows XPS spectra of PVC. The binding energies (BEs) of the peaks in the spectra were referred to that of the 1s electrons in carbonaceous carbon (284.6 eV.) [59].

Analyses by XPS were undertaken using a Microtech - ESCA 3000 Spectrometer employed with a base pressure of  $2 \times 10^{-8}$  Pa, using Mg  $K\alpha$  radiation, and achieving a resolution of about 0.8 eV. Shirley background corrections were used. For virgin PVC the following peaks were observed in the spectra: C 1s located in 291 eV, Cl 2s in 277 eV and O 1s in 538 eV. After fluorination, C 1s was set to 300 eV, Cl 2s in 280 eV, O 1s in 540 eV and F 1s in 695 eV. After nitrogen ion implantation, C 1s was located at 292 eV, Cl 2s reduced to 274 eV, O 1s at 538, and a N 1s was located at 408 eV [25]. After the treatment, XPS analysis revealed the following: carbon, oxygen, nitrogen and chlorine at, respectively, 52 at.(%), 33 at.(%), 12 at.(%) and 3 at.(%). In this situation,  $\theta$  changed from  $9^\circ$  (immediately after the treatment) to  $102^\circ$  after 30 days.

PVC is composed of about (50 at.%) carbon, (38 at.%) chlorine and few percent hydrogen [25]. As hydrogen is not detected by XPS, the atomic concentrations obtained for the virgin PVC are consistent. A small amount (~11 at.%) of oxygen is detected even in the as-received material [60]. After

the fluorination treatment the oxygen content did not change, except for the cathode configuration at 100 W, where the oxygen concentration 30 days after treatment was only 3 at. (%). Nevertheless, substantial fluorine incorporation was observed, while chlorine was removed, (virgin PVC contained 38 at. (%) Cl, and after SF<sub>6</sub> bombardment, this had decreased to about 2 at. (%).

These results support the explanation of the wettability and of the fluorination mechanism [25]. Substitution of hydrogen atoms in hydrocarbons by fluorine atoms decreases their surface energy because of the strong covalence and small polarizability of the C-F bonds. The surface energy of a material depends on the character of terminal groups, and decreases in order -CH<sub>2</sub> → -CH → -CF → -CF<sub>3</sub>. The surface energy of a solid surface is proportional to the surface fluorine atomic ratio. Nevertheless, the presence of fluorinated groups (CF, CF<sub>2</sub> and CF<sub>3</sub>) and the subsequent surface energy decrease are not enough to reach superhydrophobicity. Flat surfaces terminated with -CF<sub>3</sub> groups, which have the lowest free energy, exhibit a maximum contact angle of around 120° [60].

On the other hand, when nitrogen ions were implanted into the surface of PVC, the oxygen content increased, from 11 at. % to 33 at. %. It is believed that residual oxygen bonds with active sites on the surface caused by ion bombardment. After nitrogen plasma immersion ion implantation the surface composition was as follows: (52% C), (33%O), (12% N) and (3% Cl). For sample Nit1 (PIII), hydrophilization may be caused by the formation of oxygen-containing groups [25]. The high concentration of oxygen is consistent with the reduction in  $\theta$ . The binding Energy of O 1s observed for virgin PVC and PVC treated with nitrogen is the same: 538 eV. Under these conditions there is expected to be a high degree of bond fragmentation and the emission of species from the solid. As hydrogen and chlorine atoms are side groups in PVC, they are very prone to be lost upon bombardment [25]. Carbon atoms can also be ejected and O incorporation can be observed. Free radicals generated by Cl and H emission can react with atmospheric H<sub>2</sub>O and O<sub>2</sub>, thereby incorporating oxygen groups.

Energy calibration and background correction in XPS have been thoroughly studied and the subject is well covered in many textbooks [61]. From the practitioner point of view, the essential point to bear in mind is that the particular choice of background function has a direct effect on the peak areas (and hence the extracted concentrations). The simplest background type is a line drawn between the data points on the high and low BE sides of the peak. Although very convenient, the linear background lacks a theoretical justification. Linear background can be sufficient for wide-band gap materials (specially for polymers) [62], in which case the photoelectron energy losses associated with the presence of valence electrons occur several eV away from the no-loss line. As a result, the background intensities on the low and high BE sides of the peak are very similar, hence, the error due to the arbitrary selection of background end points is minimized. In contrast, for other classes of materials the uncertainty related to the selection of background

TABLE 5

Synthesis of the results obtained by treatment of the surface of the commercial polymers for the PI and PIII techniques.  $\theta$  indicates the contact angle,  $\theta$  (t) indicates stability upon ageing,  $R_{\text{rms}}$  Surface Roughness (root mean square) via Atomic Force Microscopy,  $T$  ( $\lambda$ ), indicates the optical transmittance in the visible region and B the gas barrier.  $T_{\text{H}}$  and  $T_{\text{C}}$  stand for hot and cold substrates.

Thermodynamic condition	$T_{\text{H}}$ (hot sample holder)		$T_{\text{C}}$ (cooled sample holder)	
	$\text{SF}_6$ plasma	$\text{N}_2$ plasma	$\text{SF}_6$ plasma	$\text{N}_2$ plasma
$\theta$	Hydrophobic except on PIII	Hydrophilic	Hydrophobic	Hydrophilic
$\theta$ (t)	Unstable	Unstable	Stable	Stable
Chemical structure or composition	a-C:F:H	a-C:H:O	a-C:F:H	a-C:H:O
$R_{\text{rms}}$	Moderately rough	Softly rough	Smooth	Smooth
$T$ ( $\lambda$ )	Subtle alteration	Low at visible	High at visible	High at visible
B (gas barrier)	–	–	–	Considerably high

end points may be significant. More advanced, and also more popular, is Shirley background correction [63]. Table 5 summarizes the results obtained.

Numerous authors also reported excellent results of wettability for several types of polymers including polyethylene terephthalate [64–66], polyether-sulphone [67,68], polyphenylene sulphide [69], polystyrene [70,71], polyvinylchloride [72,73], polymethyl methacrylate [74], cellulose [75–77] etc, and the treated polymers found a wide spectrum of applications in science and industry.

The limitations of cold plasma treatment are presented. The modification of polymer surfaces with cold plasma processing may not be permanent over extended periods. Because of the minimization of the free surface enthalpy, dynamic processes are observed on all functionalized surfaces which fade the initial modification effect [78]. The loss of beneficial attributes derived from cold plasma processing of polymers over time is often called “ageing”. For example, a loss in hydrophilicity is observed for treated polymeric films when stored. This is referred to as hydrophobic recovery. Such effects are attributed primarily to inward-diffusion, agglomeration or sublimation of “Low Weight Organic Molecules”, the reorientation of polymer chains, whereby covalently bonded polar groups become “buried” beneath the outer surface; and migration of additives from the bulk towards the surface [78].

Ageing effects are significant when the power input to the plasma and process times are both low. For the aforementioned example, this means insignificant changes in the surface roughness, i.e. less etching [78]. Conversely, where intermediate to high doses of plasma discharges are employed,

a further post-processing decrease in contact angle occurs [78]. Hence, it was demonstrated, as alternative, to use a cooling system on sample holder may minimize the effects of ageing, and then make more stable wetting properties.

From literature, it is possible to observe a wide spectrum of surface treatments and surface functionalizations to introduce, a certain formation of reactive radicals as plasma products to substrate surface, aiming to transform the surface characteristics from hydrophilic to hydrophobic using fluorine plasma, or even aiming to transform the surface characteristics from hydrophobic to hydrophilic [79,80], in our case, using nitrogen plasma.

#### 4 CONCLUSIONS

The present work contemplated the study of the superficial modification of the PVC, PET and LDPE polymers, treated by plasma techniques. The Tc condition (samples treated without sample holder cooling) gave the most stable properties.

The contact angle measurements showed an increase in the hydrophobic character for the fluorine treated polymers (whose surface became similar to Teflon, according to BRASKEM a hydrophobic material  $\Theta = 126^\circ$ ) with extreme values of contact angle observed for the PVC, reaching ~ up to  $140^\circ$ , in contrast, samples treated with nitrogen, became hydrophilic with angles close to  $\sim 1^\circ$ . Exposure of the fluorine-containing plasma polymer surface is capable of replacing hydrogen atoms with fluorine atoms.

Exposure of the polymer surface to nitrogen plasmas caused the surface with intermediate wettability to become hydrophilic. Surface modification is explained by the incorporation of functional groups such as C-OH (alcohol), -COOH- (hydroperoxide), -HC=O (aldehyde), C=O (carbonyl), -COC=O (Ester), -COO-, HOC = O (acid) and  $\text{NH}_2$  (amine), through reaction at the polymer surface by active plasma species.

#### 5 ACKNOWLEDGMENTS

The reported here was funded in part by the “Coordenação de Aperfeiçoamento de Pessoal de Nível Superior (CAPES) – Finance Code 001.

#### REFERENCES

- [1] Feng X.J. and Jiang L., Design and creation of superwetting/antiwetting surfaces. *Advanced Materials* 18 (2006), 3063–3078.
- [2] Liu, K.S., Tian Y. and Jiang L., Bio-inspired superoleophobic and smart materials: Design, fabrication, and application. *Progress in Materials Science* 58(4) (2013), 503–564.

- [3] Sant'Ana P.L. *Polímeros Tratados a Plasma Para Dispositivos e Embalagens*. Portugal: Novas edições académicas. 2019.
- [4] Senarathna R.M.D.M., Wanniarachchi W.K.I.L., Jayawardhana S. and Rathnaweera D.R. Development of a Low-cost Automated Micro Dispense Digital Goniometric Device with Drop Shape Analysis. Moratuwa Engineering Research Conference (MERCon), 2018. 4th International Multidisciplinary Engineering Research Conference May 30 – June 1 2018, University of Moratuwa, Sri Lanka.
- [5] Yuan Y. and Lee T.R., Contact Angle and Wetting Properties. In: Bracco G., Holst B. (Eds.) *Surface Science Techniques. Springer Series in Surface Sciences: Volume 51*. Berlin, Germany: Springer. 2013.
- [6] Quéré D., Wetting and roughness. *Annual Review of Materials Research* **38** (2008), 71–99.
- [7] Bico J., Thiele U. and Quéré D., Wetting of textured surfaces. *Colloids and Surfaces A: Physicochemical and Engineering Aspects* **206**(1–3) (2002), 41–46.
- [8] Arefi F., Andre V., Montazer-Rahmati P., Amouroux J., Plasma polymerization and surface treatment of polymers. *Pure and Applied Chemistry* **64**(5) (1992), 715–723.
- [9] D'Agostino R., Favia P., Fracassi F., *Plasma Processing of Polymers*. Netherlands: Springer. 1997.
- [10] Kharitonov A.P., Simbirtseva G.V., Tressaud A., Durand E., Labrugère C. and Dubois M., Comparison of the surface modifications of polymers induced by direct fluorination and rf-plasma using fluorinated gases. *Journal of Fluorine Chemistry* **165** (2014), 49–60.
- [11] Irena G., Bryjak M., Kujawski J., Wolska J. and Kujawa J., Plasma deposited fluorinated films on porous membranes. *Materials Chemistry and Physics* **151** (2015), 233–242.
- [12] Ensinger W., Plasma immersion ion implantation for metallurgical and semiconductor research and development. *Nuclear Instruments and Methods in Physics Research Section B: Beam Interactions with Materials and Atoms* **120**(1–4) (1996) 270–281.
- [13] Brown I.G., Anders A., Anders S., Dickinson M.R. and MacGill R.A., Metal ion implantation: conventional versus immersion. *Journal of Vacuum Science and Technology B* **12** (1994), 823.
- [14] Brutscher J., Gunzel R. and Moller W., Plasma immersion ion implantation using pulsed plasma with dc and pulsed high voltages. *Surface and Coatings Technology* **93**(2–3) (1997) 197–202.
- [15] Popok V.N., Khaibullin R.I., Tóth A., Beshliu V., Hnatowicz V. and Mackova A., Compositional alteration of polyimide under high fluence implantation by  $\text{Co}^+$  and  $\text{Fe}^+$  ions. *Surface Science* **532–535** (2003), 1034–1039.
- [16] Sant'Ana P.L., Bortoleto, J.R.R., Cruz N.C., Rangel E.C., Durrant, S.F., Study of Wettability and optical transparency of PET polymer modified by plasma immersion techniques. *Revista Brasileira de Aplicações de Vácuo* **36**(2) (2017), 68–74.
- [17] Sant'Ana P.L., Prestes S.M.D., Mancini S.D., Rangel R.C., Bortoleto J.R.R., da Cruz N.C., Rangel E.C. and Durrant S. F., Análise comparativa entre o grau de molhabilidade dos polímeros reciclados PVC e PET tratados por imersão ou deposição de filmes orgânicos em plasmas fluorados. *Revista Brasileira de Aplicacoes de Vacuo* **37**(3) (2019), 120–128.
- [18] Sant'Ana P.L., Bortoleto J.R.R., Cruz N.C., Rangel E.C., Durrant S.F., Botti L.M.C., dos Anjos C.A.R., Medeiros, E.A. and Soares, N.F. Surface properties of PET polymer treated by plasma immersion techniques for food packaging. *International Journal of Nano Research* **1**(1) (2018), 33–41.
- [19] Sant'Ana P.L., Bortoleto, J.R.R., Nilson C.C., Elidiane C.R., Durrant S.F., Botti L.M.C., Anjos C.A.R., Medeiros E.A.A., Soares N.F., Azevedo S., Teixeira V., Carneiro J., and Silva C.I., Surface properties and morphology of PET treated by plasma immersion ion implantation for food packaging. *Nanomedicine & Nanotechnology* **3**(3) 1–13.
- [20] Sant'Ana P.L., Bortoleto J.R.R., Cruz N.C., Rangel E.C., Durrant S.F., Botti L.M.C., dos Anjos C.A.R., Medeiros, E.A. and Soares, N.F. Surface properties of PET polymer treated by plasma immersion techniques for food packaging. *International Journal of Nano Research* **1**(1) (2018), 33–41.

- [21] Sant'Ana P.L., Bortoleto J.R.R., Cruz N.C., Rangel E.C., Durrant S.F., Botti L.M.C., Rodrigues Anjos C.A., Azevedo S., Teixeira V., Silval C.I., Carneiro J., Medeiros E.A. and de Fatima Soares N.F., Surface properties and morphology of PET treated by plasma immersion ion implantation for food packaging. *Nanomedicine and Nanotechnology* **3**(3) (2008), 000145.
- [22] Rokka J. and Uusitalo L., Preference for green packaging in consumer product choices - Do consumers care? *International Journal of Consumer Studies* **32**(5) (2008), 516–525.
- [23] Isa S.M., and Yao P.X., Investigating the preference for green packaging in consumer product choices: A choice-based conjoint approach. *Business Management Dynamics* **3**(2) (2013), 84–96.
- [24] Vukušić T., Vesel A., Holc M., Šćetar M., Jambrak A.R. and Mozetic M., Modification of physico-chemical properties of acryl-coated polypropylene foils for food packaging by reactive particles from oxygen plasma. *Materials* **11**(3) (2018), 372.
- [25] Sant'Ana P.L., *Polymers Treated By Plasma for Optical Devices and Food Packaging*. Republic of Moldova: Scholar's Press. 2018.
- [26] Lee L-H., Effect of Surface Energetics on Polymer Friction and Wear. In: Lee L-H. (Ed) *Advances in Polymer Friction and Wear*. Boston, MA, USA: Springer US, p. 31–68, 1974.
- [27] Tirrell M., Measurement of interfacial energy at solid polymer surfaces. *Langmuir* **12**(19) (1996), 4548–4551.
- [28] Sant'Ana P.L., Bortoleto J.R.R., Cruz N.C., Rangel E.C. and Durrant S.F., Study of wettability and optical transparency of PET polymer modified by plasma immersion techniques *Revista Brasileira de Vácuo* **16**(2) (2017), 68–74.
- [29] Chu P.K., Recent developments and applications of plasma immersion ion implantation (PIII). *Journal of Vacuum Science and Technology B* **22**(1) (2004), 289–96.
- [30] Chu P.K., Tang B.Y., Wang L.P., Wang X.F., Wang S.Y. and Huang N., Third-generation plasma immersion ion implanter for biomedical materials and research. *Review of Scientific Instruments* **72**(3) (2001), 1660–1665.
- [31] Guruvanket S., Rao G.M., Komath M. and Raichur A.M., Plasma surface modification of polystyrene and polyethylene. *Applied Surface Science* **236**(1–4) (2004), 278–284.
- [32] Triandafillu K., Balazs D.J., Aronsson B.O., Descouts P., Quoc P.T., Delden C.V., Mathieu H.J. and Harms H. Adhesion of pseudomonas aeruginosa strains to untreated and oxygen-plasma treated poly(vinyl chloride) (PVC) from endotracheal intubation devices. *Biomaterials* **24**(8) (2003), 1507–1518.
- [33] Park Y.W. and Inagaki N., Surface modification of poly (vinylidene fluoride) film by remote Ar, H<sub>2</sub>, and O<sub>2</sub> plasmas. *Polymer* **44**(5) (2003), 1569–1575.
- [34] Junkar I., Cvelbar U., Vesel A., Hauptman N. and Mozetic M., The role of crystallinity on polymer interaction with oxygen plasma. *Plasma Process and Polymers* **6** (2009), 667–675.
- [35] Kim Y., Lee Y., Han S. and Kim K.J., Improvement of hydrophobic properties of polymer surfaces by plasma source ion implantation. *Surface and Coatings Technology* **200**(16–17) (2007), 4763–4769.
- [36] Chuang M.J., Carbon tetrafluoride plasma modification of polyimide: A method of in-situ formed hydrophilic and hydrophobic surfaces. *Surface and Coatings Technology* **203**(23) (2009), 3527–3532.
- [37] Zanini S., Massini P., Mietta M., Grimoldi E. and Riccardi C., Plasma treatments of PET meshes for fuel–water separation applications *Journal of Colloid and Interface Science* **322**(2) (2008), 566–571.
- [38] Korotkov R.Y., Goff T. and Ricou P., Fluorination of polymethylmethacrylate with SF<sub>6</sub> and hexafluoropropylene using dielectric barrier discharge system at atmospheric pressure. *Surface and Coatings Technology* **201**(16–17) (2007), 7207–7215.
- [39] Salapare H.S.III, Guittard F., Noblin X., Taffin de Givenchy E., Celestini F. and Ramos H.J., Stability of the hydrophilic and superhydrophobic properties of oxygen plasma-treated poly(tetrafluoroethylene) surfaces. *Journal of Colloid and Interface Science* **39**(6) (2013), 287–292.
- [40] Salapare H.S.III, Darmanin T. and Guittard F., Reactive-ion etching of nylon fabric meshes using oxygen plasma for creating surface nanostructures. *Applied Surface Science* **356** (2015), 408–415.

- [41] Kikani P., Desai B., Prajapati S., Arun P., Chauhan N. And Nema S.K., Comparison of low and atmospheric pressure air plasma treatment of polyethylene. *Surface Engineering* **29**(3) (2013), 211–221.
- [42] Encinas N., Abenojar J. and Martinez. M.R., Development of improved polypropylene adhesive bonding by abrasion and atmospheric plasma surface modifications. *International Journal of Adhesion and Adhesives* **33** (2012), 1–6.
- [43] Aflori M., Drobota M., Dimitriu D., Stoica I., Simionescu B. and Harabagiu V., Collagen immobilization on polyethylene terephthalate surface after helium plasma treatment. *Materials Science and Engineering B* **178**(19) (2013), 1303–1310.
- [44] Resnik M., Zaplotnik R., Mozetic M. and Vesel A., Comparison of SF<sub>6</sub> and CF<sub>4</sub> plasma treatment for surface hydrophobization of PET polymer. *Materials* **11**(2) (2018), 311.
- [45] Yasuda H., *Luminous chemical vapor deposition and interface engineering*. New York, NY, YSA: Marcel Dekker. 2005.
- [46] Rangel E.C., Gadioli G.Z. and Cruz N.C., Investigations on the stability of plasma modified silicene surfaces. *Plasmas and Polymers* **9**(1) (2004), 35–48.
- [47] Akishev Y.S., Grushin M.E., Drachev A.I., Karalnik V.B., Petryakov A.V. and Trushkin N.I., On Hydrophilicity ageing of PP and PET films induced by ultraviolet radiation and hydrogen atoms. *The Open Plasma Physics Journal* **6** (2013), 19–29.
- [48] Al-Etaibi A., Alnassar H. and El-Asary M., Dyeing of polyester with disperse dyes: Part 2. Synthesis and dyeing characteristics of some azo disperse dyes for polyester fabrics. *Molecules* **21**(7) (2016), 855.
- [49] Drobota M., Aflori M. and Barboiu V., Protein immobilization on poly (ethylene terephthalate) films modified by plasma and chemical treatments. *Digest Journal of Nanomaterials and Biostructures* **5**(1) (2010), 35–45.
- [50] Sant’Ana P.L., Bortoleto J.R.R., Elidiane C.R., Nilson C.C., Durrant S.F., Botti L.C.M., dos Anjos C.R., Teixeira V., Azevedo S., Silva C.I., Soares, N.F.F. and Medeiros E.A.A., Surface properties of PET polymer treated by plasma immersion techniques for food packaging. *International Journal of Nano Research* **1** (2018), 33–41.
- [51] Tibbit, J. M., Bell A. T., and Shen, M. Effects of reaction conditions on the structure of plasma-polymerized ethylene. *Journal of Macromolecular Science: Part A – Chemistry* **11**(1) (1977), 139–148.
- [52] Rangel, R.C.C., *Aplicação do Eletrocapilaridade na Manipulação de Microgotas*. 2008. 87 f. Dissertação (mestrado) - Universidade Estadual Paulista, Faculdade de Ciências de Bauru, 2008.
- [53] Dong H. and Bell T., State-of-the-art overview. Ion beam surface modification of polymer towards improving tribological properties. *Surface and Coating Technology* **111**(1) (1999), 29–40.
- [54] Pandiyara K. N., Selvarajan V., Heeg J., Junge F., Lampka A., Barfels T., Wienecke M., Rhee Y. H., and Kim H. W., Influence of bias voltage on diamond like carbon (DLC) film deposited on polyethylene terephthalate (PET) film surfaces using PECVD and its blood compatibility. *Diamond and Related Materials* **19**(7–9) (2010), 1085–1092.
- [55] Sakudo N., Mizutani D., Ohmura Y., Endo H., Yoneda R., Ikenaga N., and Takikawa H., Surface modification of PET film by plasma-based ion implantation. *Nuclear Instruments and Methods in Physics Research Section B: Beam Interactions with Materials and Atoms* **206** (2003), 687–690.
- [56] Prestes, S.M.D. and Mancini S.D., Plasma treatment to improve the surface properties of recycled post- consumer PVC. *Plasma Processing and Polymers* **12** (2015), 456–465.
- [57] Foerch R., Kill G. and Walzak M. Plasma surface modification of polypropylene: short-term vs. long-term plasma treatment. *Journal of Adhesion Science and Technology* **7** (1993), 1077–1089.
- [58] Sant’Ana P.L., Prestes S.M.D., Mancini S.D., Rangel R.C.C., Bortoleto J.R.R., da Cruz N.C., Rangel E.C. and Durrant S.F., Análise comparativa entre o grau de molhabilidade dos polímeros reciclados PVC e PET tratados por imersão ou deposição de filmes orgânicos em plasmas fluorados. *Revista Brasileira de Aplicacoes da Vacuo* **37**(3) (2019), 120–128.

- [59] Cruz S.A., Zanin M., Nascente P.A.P. and Bica de Moraes M.A. Superficial modification in recycled PET by plasma etching for food packaging. *Journal of Applied Polymer Science* **115** (2010), 2728–2733.
- [60] Rangel E. C., dos Santos N. M., Bortoleto J. R. R., Durrant S. F., Schreiner W. H., Honda R. Y., Rangel R. C. C. and da Cruz N. C., Treatment of PVC using an alternative low energy ion bombardment procedure. *Applied Surface Science* **258** (2006), 1854–1861.
- [61] Tougaard S., Quantification of Nano-Structures by Electron Spectroscopy. In: D. Briggs D. and Grant J.T. (Eds.), *Surface Analysis by Auger and X-ray Photoelectron Spectroscopy*. Chichester, UK: IM Publications. 2003. **12**, pp. 295–344.
- [62] Beamson G. and Briggs D., *High Resolution XPS of Organic Polymers*, The Scienta ESCA 300 database. Chichester, UK: John Wiley & Sons. 1992.
- [63] Greczynski G. and Hultman L. X-ray photoelectron spectroscopy: Towards reliable binding energy referencing, *Progress in Materials Science* **107** (2020), 100591.
- [64] Junkar I., Cvelbar U., Vesel A., Hauptman N. and Mozetic M., The Role of Crystallinity on Polymer Interaction with Oxygen Plasma, *Plasma Processes and Polymers* **6**(10) (2009), 667–675.
- [65] Vesel A., Mozetic M. and Zalar A., XPS study of oxygen plasma activated PET, *Vacuum* **82**(2) (2008), 248–251.
- [66] Vesel A., Junkar I., Cvelbar U., Kovac J. and Mozetic M., Surface modification of polyester by oxygen- and nitrogen-plasma treatment, *Surface and Interface Analysis* **40**(11) (2008), 1444–1453.
- [67] Vrlinic T., Vesel A., Cvelbar U., Krajnc M. and Mozetic M., Rapid surface functionalization of poly(ethersulphone) foils using a highly reactive oxygen-plasma treatment, *Surface and Interface Analysis* **39**(6) (2007), 476–481.
- [68] Feng J., Wen G., Huang W., Kang E. and Neoh K.G., Influence of oxygen plasma treatment on poly(ether sulphone) films, *Polymer Degradation and Stability* **91** (1) (2005), 12–20.
- [69] Cvelbar U., Mozetic M., Junkar I., Vesel A., Kovac J., Drenik A., Vrlinic T., Hauptman N., Klanjsek – Gunde M., Markoli B., Krstulovic N., Milosevic S., Gaboriau F. and Belmonte T., Oxygen plasma functionalization of poly(*p*-phenylene sulphide), *Applied Surface Science* **253** (21) (2007), 8669–8673.
- [70] Vesel A. Modification of polystyrene with a highly reactive cold oxygen plasma, *Surface and Coatings Technology* **205**(2) (2010), 490–497.
- [71] Wang M. J., Chang Y. I. and Poncin-Epaillard F. Acid and basic functionalities of nitrogen and carbon dioxide plasma-treated polystyrene, *Surface and Interface Analysis* **37** (2005), 348.
- [72] Asadinezhad A., Novak I., Lehocky M., Bilek F., Vesel A., Junkar I., Saha P. and Popelka A. Polysaccharides coatings on medical-grade PVC: A probe into surface characteristics and the extent of bacterial adhesion, *Molecules* **15**(2) (2010), 1007–1027.
- [73] Asadinezhad A., Novak I., Lehocky M., Sedlarik V., Vesel A., Junkar, Saha P., and Chodak I., A physicochemical approach to render antibacterial surfaces on plasma-treated medical-grade PVC: Irgasan Coating, *Plasma Processes and Polymers* **7**(6) (2010), 504–514
- [74] Vesel A., Mozetic M., Hladnik A., Dolenc J., Zule J., Milosevic S., Krstulovic N., Klanjsek – Gunde M. and Hauptman N., Modification of ink-jet paper by oxygen-plasma treatment, *Journal of Physics D: Applied Physics* **40**(12) (2007), 3689–3696.
- [75] Gorjanc M., Bukosek V., Gorensek M. and Vesel A. The influence of water vapor plasma treatment on specific properties of bleached and mercerized cotton fabric, *Textile Research Journal* **80**(6) (2010), 557–567.
- [76] Jovancic P., Jocic D., Radetic M., Topalovic T. and Petrovic Z.L. The influence of surface modification on related functional properties of wool and hemp. *Current Research Advances in Material Processing* **494** (2005), 283–290.
- [77] Vesel A., Mozetic M., Strnad S., Stana–Kleinschek K., Hauptman N. and Persin Z. Plasma modification of viscose textile, *Vacuum* **84**(1) (2010), 79–82.



- [78] Pankaj S.K., Bueno Ferrer C., Misra N.N., Milosavljevic V., O'Donnell, C.P.O., Bourke P., Keener K.M. and Cullen P.J. Applications of cold plasma technology in food packaging, *Trends in Food Science & Technology* **35** (2014), 5–17.
- [79] Kuo Y.-L., Chang K.-H and Chiu C., Carbon-free SiO<sub>x</sub> ultrathin film using atmospheric pressure plasma jet for enhancing the corrosion resistance of magnesium alloys, *Vacuum*, **146** (2017), 8–10.
- [80] Audronis M., Hinder S.J., Mack P., Bellido-Gonzalez V., Bussery D., Matthew A., and Baker M.A., A comparison of reactive plasma pre-treatments on PET substrates by Cu and Ti pulsed-DC and HIPIMS discharges, *Thin Solid Films* **520**(5) (2011), 1564–1570.